한국광물학회지 제 17 권 제 3 호 (2004년 9월)
J. Miner. Soc. Korea, 17(3), 201-208 (September, 2004)

Elastic Properties of the $CaSiO_3$ - Garnet Phase

$CaSiO_3$ - 석류석 상의 탄성 특성

Young-Ho Kim (김 영 호)*

Department of Earth and Environment Science and the Research Institute of Natural Science,
Gyeongsang National University, Jinju 660-701, Korea
(경상대학교 기초과학부 지구환경과학 전공, 경상대학교 기초과학연구소)

ABSTRACT : $CaSiO_3$-garnet phase was observed in the phase transformation sequences on a natural hedenbergite, $(Ca,Fe)SiO_3$ between 14 and 24 GPa when quenched from ~1200℃. Bulk modulus K = 155 GPa, V_ϕ = 6.58 km/sec and other elastic properties of the $CaSiO_3$-garnet were obtained on the basis of the systematics of structural analogs in various garnet phases and relationship of KV_m = constant and $V_\phi M^{\frac{1}{3}}$ = constant. This quenchable garnet phase appears to be stabilized by the considerable amount of Mn and other cations, and shows a wide stability range. As one of the host minerals of Ca composition, $CaSiO_3$-garnet would be one of the important mineral phases in the mantle transition region.

Key words : hedenbergite, $CaSiO_3$-garnet phase, elastic properties, mantle transition region

요약 : 천연산 헤덴버자이트$(Ca,Fe)SiO_3$ 시료에 대해 일정한 압력 하에서 약 1200℃ 정도로 가열한 후, x-선 회절실험을 시행하였더니 14~24 GPa 압력구간에서 등축정계에 속하는 석류석 상이 관찰되었다. $CaSiO_3$-석류석 상에 대한 체적탄성률 = 155 GPa 및 V_ϕ = 6.58 km/sec 및 기타 탄성특성을 유사구조의 계통과 KV_m = 상수 및 $V_\phi M^{\frac{1}{3}}$ = 상수 관계식을 이용하여 추정하였다. 석류석 상은 천연산 헤덴버자이트에 상당량 포함되어 있는 Mn과 많은 미량원소에 의해 상당히 넓은 압력에 걸쳐 안정영역을 구축하며, 비가역적 반응을 보인다. Ca의 포용광물로 $CaSiO_3$-석류석 상은 맨틀전이대의 주요 광물상의 하나로 간주할 수 있다.

주요어 : 헤덴버자이트, $CaSiO_3$-석류석 상, 탄성특성, 맨틀전이대

*Corresponding Author (교신저자): yhkim@gsnu.ac.kr

Introduction

The system of $Ca(Mg,Fe)Si_2O_6$ is regarded as one of the important mineral phases in the Earth's mantle (Bass and Anderson, 1984; Anderson and Bass, 1986). Its importance has been enhanced by the recent estimates of the solar composition, which show the enrichment of Fe and Ca with respect to Mg, Al, and Si as compared with the previous values (Anderson, 1989). A knowledge of the physical properties and phase relations in this system at high pressures and temperatures can provide constraints for the interpretation of seismic velocities in the Earth's mantle. Several studies have been performed on hedenbergite ($(Ca,Fe)SiO_3$), an end member in this system: crystal structure refinement (Veblen and Burnham, 1970), isothermal compression (Vaidya *et al.*, 1973), thermal expansivity (Cameron *et al.*, 1973; Finger and Ohashi, 1976), elasticity (Kandelin and Weidner, 1988), molecular vibration (Sharma *et al.*, 1988), and phase transformations at high pressures and temperatures (Kim *et al.*, 1989).

Among phase transformation studies, it was found out $CaSiO_3$-garnet phase, which was stablized by the minor elements in the natural specimen (Kim *et al.*, 1989). This paper aims to report the elastic properties of this new phase and to discuss the geophysical implications.

Experiments

Hedenbergite powder sample was prepared from one of the natural mineral collections from the University of Rochester. Chemical formula of specimen was derived to be $(Ca_{0.93}Fe_{0.61}Mn_{0.34}Mg_{0.08}Na_{0.01}Zn_{0.02}Al_{0.003})Si_2O_6$ by Klein and Hurlbut's procedure (1985) using the electron microprobe analyses (Table 1). Lattice parameters of this starting specimen were determined by x-ray diffraction (XRD) method using Debye-Scherrer camera: $a = 9.777$ Å, $b = 8.940$ Å, $c = 5.260$ Å, $\beta = 104.8°$ (ASTM 16-701; $a = 9.850$ Å, $b = 9.020$ Å, $c = 5.260$ Å, $\beta = 104.2°$). Comparing these, a- and b-axes of sample are shorter than those in ASTM. This discrepancy might be related to the chemical composition difference, which shows the high content of Mn in the present sample.

Sample was compressed up to a high pressure using a gasketted Bassett-type diamond anvil cell (DAC) and then heated with an YAG laser heating system at 1200℃. Both pressure and temperature determination procedures in this study were same as the previous studies given elsewhere (Ming and Bassett, 1974; Kim *et al.*, 1989; Kim, 1994). Treated sample in this way was unloaded to 0.1 MPa (i.e., 1 atmospheric pressure), and transferred to the modified Debye-Scherrer camera, then x-rayed using Ni-filtered Cu-K_α radiation.

Results and Discussions

Phase Sequences

In this experiment, the compressed laser-heated sample was quenched to ambient temperature, unloaded to 0.1 MPa, and then x-rayed. XRD patterns from the run of 14 GPa show that there are three phases retained: garnet phase, ɣ-spinel phase and stishovite phase (Table 2). As shown in Fig 1, XRD patterns of the garnet phase are in accordance with those of andradite ($Ca_3Fe_2Si_3O_{12}$). Based on the observed *d*-spacings for each phase, lattice parameter of garnet, ɣ-spinel and stishovite phases were determined to be $a = 11.872(15)$ Å, $a = 8.234(19)$ Å, and $a = 4.188(2)$ Å, $c = 2.653(3)$ Å, respectively. The calculated *d*-spacings on the basis of these lattice parameters for each phase show a very good agreement with the observed ones. The present run at 14 GPa indicates the completion of the phase transformation at this pressure and heating temperature conditions for this natural hedenbergite.

XRD data of the post-lasered sample unloaded from 18 GPa to atmospheric pressure are given in Table 3, which show more XRD lines than the previous 14 GPa run. In this run, four phases were identified and lattice parameters for

Table 1. Electron microprobe analysis of the hedenbergite

Oxide	Weight %
SiO_2	47.94
CaO	21.38
FeO	18.01
MnO	9.86
MgO	1.36
ZnO	0.66
Na_2O	0.10
Al_2O_3	0.06
total	99.37

Table 2. X-ray diffraction data of the post-lasered natural hedenbergite unloaded from ~14 GPa to 0.1 MPa

I/I0*	d(obs.), Å	phase(s)	d(calc.)**, Å
75	2.998	gt(400)	2.986
80	2.961	st(110)	2.961
100	2.656	gt(420)	2.655
55	2.531	gt(332)	2.531
60	2.485	γ-(311)	2.483
20	2.425	gt(422)	2.423
40	2.171	gt(521)	2.168
45	2.052	γ-(400)	2.059
35	1.975	st(111)	1.976
15	1.711	gt(444)	1.714
20	1.644	gt(640)	1.646
55	1.597	gt(642)/γ-(333,511)	1.587/1.585
35	1.532	st(211)	1.530
10	1.480	st(220)	1.481
25	1.458	γ-(440)	1.456

* Relative intensities were determined visually on XRD film.

** The *d*-spacings were calculated on the basis of the following lattice parameters (unit in Å): garnet; a = 11.872(15), γ-spinel; a = 8.234(19), stishovite; a = 4.188(2), c = 2.653(3)

each phase were calculated on the basis of the observed d-spacings: garnet; a = 11.900(18) Å, γ-spinel; a = 8.231(4) Å, stishovite ; a = 4.190(2) Å, c = 2.655(2) Å, wustite; a = 4.341(1) Å. XRD data from 22 GPa following the same procedure are shown in Table 4. In this run, however, three phases were identified and lattice parameters for each phase were calculated on the basis of the observed *d*-spacings: garnet; a = 11.920(14) Å, stishovite; a = 4.185(1) Å, c = 2.663(2) Å, wustite; a = 4.344(2) Å. This indicates that γ-spinel di-

Table 3. X-ray diffraction data of the post-lasered natural hedenbergite unloaded from ~18 GPa to 0.1 MPa

I/I0*	d(obs.), Å	phase(s)	d(calc.)**, Å
50	2.989	gt(400)	2.975
50	2.964	st(110)	2.963
100	2.656	gt(420)	2.661
40	2.543	gt(332)	2.537
40	2.483	γ-(311)/w(111)	2.482/2.506
15	2.429	gt(422)	2.429
5	2.335	gt(510)	2.334
10	2.241	st(101)	2.243
70	2.174	gt(521)/w(200)	2.173/2.171
20	2.058	γ-(400)	2.058
20	1.979	st(111)	1.977
20	1.931	gt(611)	1.930
5	1.873	st(210)	1.874
10	1.647	gt(640)	1.650
40	1.589	gt(642)/γ-(333,511)	1.590/1.584
35	1.532	st(211)/w(220)	1.531/1.535
15	1.479	st(220)	1.481
20	1.454	γ-(440)	1.455

* Relative intensities were determined visually on XRD film.

** The *d*-spacings were calculated on the basis of the following lattice parameters (unit in Å): garnet; a = 11.900(18), γ-spinel; a = 8.231(4), stishovite; a = 4.190 (2), c = 2.655(2), wustite; a = 4.341(1)

sproportionates and transforms into stishovite and wustite phases completely. In order to confirm this sequence, one more run was carried out from the pressure of 26 GPa (Table 5). In this run, furthermore, garnet phase disappears, and there exist only two phases of stishovite and wustite. Lattice parameters for each phase were calculated on the basis of the observed *d*-spacings: stishovite; a = 4.190(2) Å, c = 2.655(2) Å and wustite; a = 4.341(1) Å. This observation indicates that garnet phase transforms into the higher pressure phases at the some pressure between 22 and 26 GPa.

$CaSiO_3$-Garnet Phase

Zero pressure lattice parameters (i.e., a_0) of the garnet phase observed at this experiment quenched from ~1200℃ and unloaded from several high pressure conditions are shown in

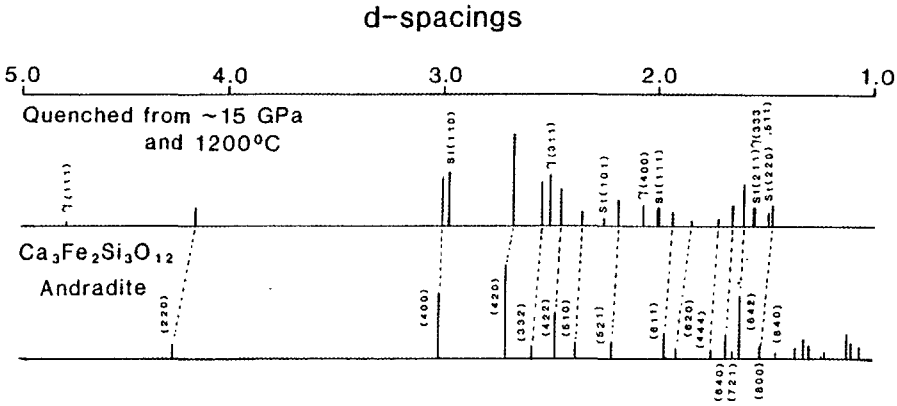

Fig. 1. Comparison of XRD patterns of between a run unloaded from ~14 GPa and the andradite garnet. γ stands for γ-spinel phase, and st does stishovite phase.

Table 4. X-ray diffraction data of the post-lasered natural hedenbergite unloaded from ~22 GPa to 0.1 MPa

I/I0*	d(obs.), Å	phase(s)	d(calc.)**, Å
60	2.987	gt(400)	2.980
60	2.959	st(110)	2.959
80	2.670	gt(420)	2.665
50	2.508	w(111)	2.508
40	2.430	gt(422)	2.433
15	2.339	gt(510)	2.338
18	2.246	st(101)	2.247
100	2.173	w(200)	2.172
30	1.981	st(111)	1.980
15	1.933	gt(611)	1.934
12	1.882	st(210)	1.872
20	1.652	gt(640)	1.653
55	1.594	gt(642)	1.593
60	1.535	st(211)/w(220)	1.531/1.536
18	1.473	st(220)	1.479

* Relative intensities were determined visually on XRD film.

** The *d*-spacings were calculated on the basis of the following lattice parameters (unit in Å): garnet; a = 11.920(14), stishovite; a = 4.185(1), c = 2.663(2), wustite; a = 4.344(2)

Table 6. There exist some discrepancies among lattice parameters according to the high pressure values. Lattice parameter appears to increase with increasing pressure. However, the large standard deviation associated with a_0 values makes the trend less clear. So, it seems to be probably independent to the quenching pressures.

Table 5. X-ray diffraction data of the post-lasered natural hedenbergite unloaded from ~26 GPa to 0.1 MPa

I/I0*	d(obs.), Å	phase(s)	d(calc.)**, Å
75	2.961	st(110)	2.959
65	2.507	w(111)	2.506
25	2.246	st(101)	2.248
100	2.174	w(200)	2.171
30	1.985	st(111)	1.980
12	1.869	st(210)	1.872
60	1.530	st(211)/w(220)	1.532/1.535
15	1.480	st(220)	1.480
8	1.306	w(311)	1.309
12	1.234	st(301)	1.236

* Relative intensities were determined visually on XRD film.

** The *d*-spacings were calculated on the basis of the following lattice parameters (unit in Å): stishovite; a = 4.190(2), c = 2.655(2), wustite; a = 4.341(1)

The average a_0 for the garnet phase is 11.894 Å. This value is comparable with those for calcium-rich garnets such as andradite (a_0 = 12.059 Å [ASTM; 10-288]) and grossular (a_0 = 11.850 Å [ASTM; 26-292]); however, it is larger than that for the iron-rich garnet (e.g., almandine, (a_0 = 11.530 Å [ASTM; 9-427])) and for the manganese-rich garnet (e.g., spessartine, (a_0 = 11.510 Å [ASTM; 10-354])). This value is also much higher than that of majorite (i.e., a_0 = 11.510 Å, Mason *et al.*, 1968; Smith and Mason, 1970; Coleman, 1977), which is a Mg-rich ABO_3-type garnet. These comparisons are extended to

Table 6. Lattice parameter of the garnet phase quenched from ~1200℃ and unloaded from several high pressure conditions

P, GPa	a, Å
14	11.872(15)
15	11.886(23)
18	11.900(18)
22	11.920(14)

Table 7. List of silicate and germanate garnets in tetragonal and cubic crystal system

Phase*	a, Å	c, Å	V, Å3	<r>(1)	Sys(2)
$MgSiO_3$	11.470	11.398	1500	0.571	Tet
$MniO_3$	11.774	11.636	1613	0.599	〃
$CaSiO_3$	11.913		1691	0.690	Cub
$Mg_3Al_2Si_3O_{12}$	11.459		1505	0.564	〃
$Fe_3Al_2Si_3O_{12}$	11.531		1533	0.571	〃
$Mn_3Al_2Si_3O_{12}$	11.612		1566	0.579	〃
$Ca_3Al_2Si_3O_{12}$	11.845		1662	0.650	〃
$Ca_3Cr_2Si_3O_{12}$	11.988		1723	0.671	〃
$Ca_3V_2Si_3O_{12}$	12.011		1733	0.678	〃
$Ca_3Fe_2Si_3O_{12}$	12.058		1753	0.679	〃
$Cd_3Al_2Si_3O_{12}$	11.820		1651	0.631	〃
$CaGeO_3$	12.514	12.358	1935	0.763	Tet
$CdGeO_3$	12.406	12.256	1886		〃
$Mn_3Ga_2Ge_3O_{12}$	12.000		1728	0.654	Cub
$Ca_3Fe_2Ge_3O_{12}$	12.320		1870	0.731	〃
$Ca_3Al_2Ge_3O_{12}$	12.112		1777	0.703	〃
$Ca_3Cr_2Ge_3O_{12}$	12.262		1844	0.724	〃
$Ca_3V_2Ge_3O_{12}$	12.320		1870	0.730	〃
$Cd_3Cr_2Ge_3O_{12}$	12.213		1822	0.705	〃
$Cd_3Fe_2Ge_3O_{12}$	12.260		1842	0.713	〃
$Mn_3Al_2Ge_3O_{12}$	11.902		1686	0.631	〃
$Mn_3Cr_2Ge_3O_{12}$	12.027		1740	0.653	〃
$Mn_3Fe_2Ge_3O_{12}$	12.087		1766	0.660	〃

(1) $\langle r\rangle = (3r_A + 2r_B + 3r_{Si})/8$, see text for explanation. Data on radius for each cation are from Shannon and Prewitt (1969).

(2) Tet; tetragonal system, Cub; cubic system

* For silicates, $MgSiO_3$ (Sawamoto, 1987), $MnSiO_3$ (Fujino *et al.*, 1986), $CaSiO_3$ (This study) and others (Novak *et al.*, 1971), and for germanates, $CdGeO_3$ (Ringwood and Major, 1967), $CaGeO_3$ (Prewitt and Sleight, 1969) and others (Galasso, 1970)

other silicate and germanate garnets (Table 7).

Elastic Properties of $CaSiO_3$-Garnet

There are many reported elastic constants on

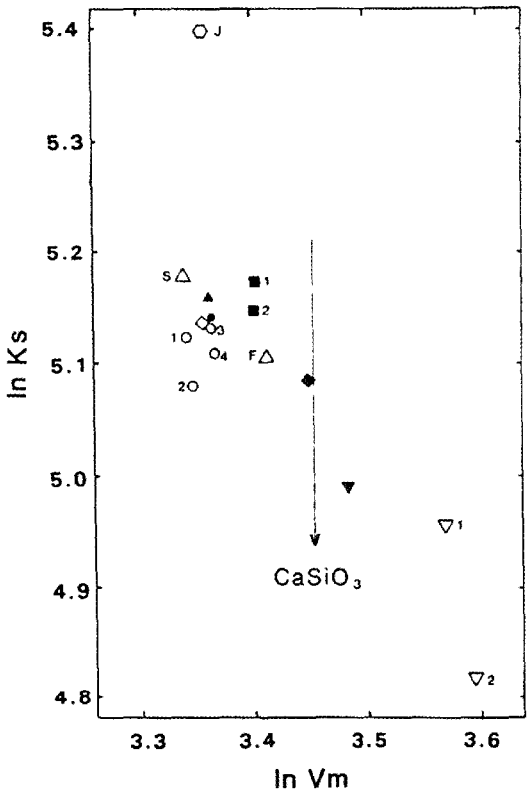

Fig. 2. K_S and V_m systematics in garnet phases. J: (Mg, Fe)SiO_3 (Jeanloz, 1981), S: $MgSiO_3$ (Sawamoto, 1987). Solid triangle: almandine from average of 5 values, solid circle: pyrope from avarage of 4 values, circles 1 and 2: spessartines, solid diamond: grossular, inverse solid triangle: andradite. All these data from Babuska *et al.*, (1978). Diamond: Al45-Py41-Gr23 (Dietrich and Arndt, 1982). Circles 1, 2, 3, and 4: Y-Py, Y-58En, Y-Al, and Y-Fs, respectively (Yagi *et al.*, 1987). Inverse triangle 1 and 2: $CdGeO_3$ and $CaGeO_3$, respectively (Liebermann, 1974). The lnV_m of $CaSiO_3$-garnet is indicated by arrow.

the various garnet phases both in cubic and in tetragonal systems (Liebermann, 1974; Babuska *et al.*, 1978; Jeanloz, 1981; Dietrich and Arndt, 1982; Fujino *et al.*, 1986; Sawamoto, 1987). From these available data (Table 8) and relationships of KV_m = constant and $V_\phi M^{\frac{1}{2}}$ = constant, the bulk modulus $K = 155$ GPa and $V_\phi = 6.58$ km/sec were obtained. Here, V_m is the molar volume, V_ϕ the hydrodynamic velocity (i.e.,

Table 8. Elasticity of garnet

Sample*	Vm (cm^3/mol)	KS (GPa)	μ (GPa)	Vφ (km/s)	VP (km/s)	Ref
Py-0	28.90	170.0	92.6	6.77	8.90	1
Py-1	28.90	171.3	92.6	6.80	8.92	1
Py-2	28.93	171.6	92.1	6.81	8.92	1
Py-A	28.91	170.8	92.0	6.77	8.88	1
Al-4	28.89	174.9	95.5	6.67	8.77	1
Al-5	29.02	175.4	96.2	6.59	8.69	1
Al-6	28.68	173.7	95.4	6.66	8.77	1
Al-X	28.91	173.4	95.9	6.63	8.77	1
Al-Y	28.81	173.6	95.6	6.61	8.74	1
Sp-1	29.46	176.4	96.5	6.50	8.55	1
Sp-2	29.44	171.8	93.3	6.41	8.41	1
Gr-1	31.48	161.6	102.6	6.65	9.02	1
An-2	32.60	147.3	92.7	6.25	8.47	1
Y-Py	28.28	167.9				2
Y-58En	28.42	161.0				2
Y-Al	28.87	169.5				2
Y-Fs	28.98	165.6				2
Al-Py-Gr	28.76	169.9				3
$CaGeO_3$	36.42	124.0	67.0			4
$CdGeO_3$	35.50	142.0	57.0			4
$(Mg, Fe)SiO_3$	28.73	221.0				5
$MnSiO_3$	30.35	164.9				6
$MgSiO_3$	28.23	177.2	101.0			7
Py	28.92	171.0	92.0			8
$CaSiO_3$	31.65	155.2	94.5	6.58	8.71	9

* Py: Pyrope, Al: Almandine, Sp: Spessartine, Gr: Grossular, An: Andradite.
1. Babuska *et al.*, 1978, 2. Yagi *et al.*, 1987, 3. Dietrich and Arndt, 1982, 4. Liebermann, 1974, 5. Jeanloz, 1981, 6. Fujino *et al.*, 1986, 7. Sawamoto, 1987, 8. Chen *et al.*, 1999, 9. This study

$\sqrt{V_p^2 - \frac{4}{3} V_s^2}$) and M is the mean atomic weight. The relation of KV_m = constant is shown in Fig 2. The other calculated elastic properties are listed in Table 9. In all calculations, the values of majorite (Jeanloz, 1981) and germanate garnets (Liebermann, 1974) were excluded because of its trend off from the main stem and their different chemical compositions, respectively. Shear modulus was calculated from the simple linear fit of K_S with respect to μ in Table 8. The V_P and V_S were calculated from the relation; $V_P = 1.152 + 1.148\ V_\phi$ and $V_S = 1.502 + 0.522\ V_\phi$. Poisson's ratio (σ) was obtained from the relation of μ/K_S by $\sigma = (3K_S - 2\mu)/(6K_S + 2\mu)$. There is a relationship how the value of dμ/dP varies with for silicates, corundum and perovskite, expressed as $d\mu/dP = 5(\mu/K_S) - 1.40$ (Sawamoto, 1987). From the calculated μ/K_S, dμ/dP value was estimated.

Ionic Sites in Garnet Structure

In tetragonal garnet of $MnSiO_3$, Mn resides at the cubic sites (C_1 and C_2), Si at the tetragonal sites (T_1, T_2, and T_3), and each one of Mn and Si at octahedral sites (O_1 and O_2), respectively (Fujino *et al.*, 1986). This indicates that Mn and Si atoms are fully ordered into different octahedral sites together. These regular ordering of cations in octahedral sites were observed in $CaGeO_3$ and $CdGeO_3$ (Prewitt and Sleight, 1968). The mode of cation ordering for non-cubic garnet structure depends on the difference in ionic radius between the two kinds of octa-

Table 9. Physical properties of cubic $CaSiO_3$-garnet phase

Properties	Values*	Rem
K_S (GPa)	155.2	
μ (GPa)	94.5	
ρ (gr/cm^3)	3.667	
V_m (cm^3/mol)	31.65	
M (gr)	23.23	
V_P (km/s)	8.71	
V_S (km/s)	4.94	
V_ϕ (km/s)	6.58	
σ	0.247	
dK_S/dP	5	1
$d\mu/dP$	1.64	

* All values are estimated from the garnet systematics except 1.
1. assumed value

hedral cations. On the other hand, the cubic garnet of majorite has a disordered structure with a mixing of Mg and Si ions in the octahedral sites. Therefore, $CaSiO_3$-garnet is supposed to have a disordered mixing of Ca and Si ions in the octahedral sites.

It is worth while considering the ionic preference sites in garnet structures of the minor cations such as Na^+, Mn^{2+}, Fe^{2+}, Mn^{3+}, Fe^{3+}, and Al^{3+} identified in a natural hedenbergite. The Ca^{2+} resides in the cubic sites and Si^{4+} in the tetrahedral sites exclusively. It is most likely that almost of those minor ions reside at the octahedral sites with disordered mixing Ca and Si ions.

Geophysical Implications

Garnet structured phase has not been reported in the end member $CaSiO_3$, at high pressures and high temperatures. In this study, a natural hedenbergite with a considerable amount of Mn and other cations exhibits a wide stability range for the garnet phase (i.e., more than 8 GPa). In view of the improved amount of Ca, as a host mineral of Ca, Ca-rich garnet phase can not be ruled out as one of the important mineral phases in the Earth transition region between 400 and 660 km depth.

Conclusions

$CaSiO_3$-garnet phase was observed in the phase transformation sequences under high pressure and temperature conditions on a natural hedenbergite, $(Ca_{0.93}Fe_{0.61}Mn_{0.34}Mg_{0.08}Na_{0.01}Zn_{0.02}Al_{0.003})Si_2O_6$. This garnet phase is quenchable, and stabilized by the considerable amount of manganese ion and other minor cations existed in the sample.

From both the systematics of structural analogs in various garnet and relationship of KV_m = constant as well as $V_\phi M^{\frac{1}{2}}$ = constant, the bulk modulus $K = 155$ GPa and $V_\phi = 6.58$ km/sec of the $CaSiO_3$-garnet observed in this natural hedenbergite were obtained.

No garnet phase has been reported in the end member $CaSiO_3$, at high pressures and high temperatures. Garnet phase appears to be stabilized by considerable amount of Mn and other cations, and shows a wide stability range (i.e., between 14 and 24 GPa). As one of the host minerals of Ca composition, $CaSiO_3$-garnet would be one of the important mineral phases in the Earth transition region.

Acknowledgments

The writer is grateful to Prof. Li Chung Ming at the University of Hawaii at Manoa for his advice and suggestions during experiment and analyses of data. Also thanks to reviewers, Dr. Youn Joong Kim and Prof. Sung Keun Lee for their contribution to improve the contents of this paper. All figures were prepared by Mr. Hwang Gil Chan, at the Mineral Physics Lab. Gyeongsang National University.

References

Anderson, D.L. (1989) Composition of the Earth. Science, 243, 367-370.

Anderson, D.L. and Bass, J.D. (1986) Transition region of the Earth's upper mantle. Nature, 320 (6060), 321-328.

Babuska, V., Fiala, J., Kumazawa, M., Ohno, I., and Sumino, Y. (1978) Elastic properties of garnet

solid-solution series. Phys. Earth & Planet. Int., 16, 157-176.

Bass, J.D. and Anderson, D.L. (1984) Composition of the upper mantle, geophysical tests of two petrological models. Geophys. Res. Lett., 11, 237-240.

Cameron, M., Sueno, S., Prewitt, C.T., and Papike, J.J. (1973) High-temperature crystal chemistry of acmite, diopside, hedenbergite, jadeite, spodumene and ureyite. Am. Mineral., 58, 594-618.

Chen, G., Cooke Jr. J.A., Gwanmesia, G.D., and Liebermann, R.C. (1999) Elastic wave velocities of $Mg_3Al_2Si_3O_{12}$-pyrope garnet to 10 GPa. Am. Mineral., 84, 384-388.

Coleman. L.C. (1977) Ringwoodite and majorite in the Catherwood meteorite. Can. Mineral., 15, 97-101.

Dietrich, P. and Arndt, J. (1982) Effects of pressure and temperature on the physical behavior of mantle-relevant olivine, orthopyroxene and garnet. In: Schreyer, W. (ed). High-pressure researches in geosciences, 293-306.

Finger, L.W. and Ohashi, Y. (1976) The thermal expansion of diopside to 800℃ and a refinement of a crystal structure at 700℃. Am. Mineral., 61, 303-310.

Fujino, K., Momoi, H., Sawamoto, H., and Kumazawa, M. (1986) Crystal structure and chemistry of $MnSiO_3$ tetragonal garnet, Am. Mineral., 71, 781-785.

Galasso, F.S. (1970) Structure and properties of inorganic solids, International series of monograph in solid state physics, 7, Pergamon Press, 247-248.

Jeanloz, R. (1981) Majorite: Vibrational and compressional properties of a high-pressure phase. J. Geophys. Res., 86, 6171-6179.

Kandelin, J. and Weidner, D.J. (1988) Elastic properties of hedenbergite. J. Geophys. Res., 93, 1063-1072.

Kim, Y.H., Ming, L.C., and Manghnani, M.H. (1989) A study of phase transformation in hedenbergite to 40 GPa at 1200℃. Phys. Chem. Minerals, 16, 757-762.

Kim, Y.H. (1994) A study of phase transitions on natural diopside under high pressure. Jour. Geol. Soc. Korea, 30(2), 159-167.

Klein, C. and Hurlbut Jr., C.S. (1985) Manual of Mineralogy, after JD Dana, John Wiley & Sons. NY, pp 596.

Liebermann, R.C. (1974) Elasticity of pyroxene-garnet and pyroxene-ilmenite phase transformations in germanates. Phys Earth & Planet. Int., 8, 361-374.

Mason, B., Nelson, J., and White, Jr. J.S. (1968) Olivine-garnet transformation in a meteorite. Science, 160, 66-67.

Ming, L.C. and Bassett, W.A. (1974) Laser heating in the diamond anvil press up to 2000℃ sustained and 3000 ℃ pulsed at pressures up to 260 kilobars. Rev. Sci. Instrum., 45, 1115-1118.

Novak, G.A. and Gibbs, G.V. (1971) The crystal chemistry of the silicate garnets. Am. Mineral., 56, 791-825.

Prewitt, C.T. and Sleight, A.W. (1969) Garnet-like structures of high-pressure cadmium germanate and calcium germanate. Science, 163, 386-387.

Ringwood, A.E. and Major, A. (1967) Some high-pressure transformations of geophysical significance. Earth & Planet. Sci. Lett., 2, 106-110.

Sawamoto, H. (1987) Phase diagram of $MgSiO_3$ ar pressures up to 24 GPa and temperatures up to 2200℃: phase stability and properties of tetragonal garnet. In: Manghnani, M.H. and Syono, Y., (eds). High-pressure research in mineral physics, Terra Scientific Pub Co. Japan/Am. Geophys. Union, 209-219.

Shannon, R.D. and Prewitt, C.T. (1969) Effective ionic radii in oxides and fluorides. Acta. Cryst., B25, 925-946.

Sharma, S.K., Yoder, H.S., and Jr., Cooney, T.F. (1988) Raman spectral study of acmite and hedenbergite in crystalline and glassy states (abstract). Trans. Am. Geophys. Union, 69, 1482.

Smith, J.V. and Mason, B. (1970) Pyroxene-garnet transformation in Coorara meteorite. Science, 168, 832-833.

Vaidya, S.N. Bailey, S., Pasternak, T., and Kennedy G.C. (1973) Compressibility of fifteen minerals to 45 kilobars. J. Geophys. Res., 78, 6893-6898.

Veblen, R. and Burnham, C.W. (1970) The crystal structure of hedenbergite and ferrosilite. Can. Mineral., 10, 147.

Yagi, T., Akaoki, M., Shimomura, O., Tamai, H., and Akimoto, S. (1987) High pressure and high temperature equations of state of majorite. In: Manghnani, M.H. and Syono, Y. (eds). High-pressure research in mineral physics, Terra Scientific Pub Co. Japan/Am. Geophys. Union, 141-148.

2004년 8월 26일 원고접수, 2004년 9월 4일 게재승인.